width, $2a$, with the height, E, and mass, m, being less important. In our model for biradical decay, the width is essentially determined by how steeply the S surface falls. Introducing a well (or deepening an existing well) on S means that it initially rises and then falls, and this can increase the barrier width. Thus, **1**-Et and **1**-Me are presented with a fairly narrow barrier, through which tunneling is feasible, but **1**-Vin, **1**-EV, and **1**-Ph face too wide a barrier for tunneling. The model also nicely explains the increase in E_a on going from **1**-Et to **1**-Vin and why E for **1**-Et is smaller than 1.5 kcal/mol, the computed value of E_{S-T}.[26] Of course, at this point the model outlined in Figure 14 is strictly conjecture, and it will be interesting to see whether further examples support the basic scheme.

Conclusions

The cyclobutanediyls constitute a general class of triplet ground state, localized 1,3-biradicals. With stabilizing substituents such as vinyl or phenyl on the radical centers, the biradicals are indefinitely stable at 4 K. On warming to 20–50 K, ring closure commences, and the variation of the decay rates with temperature follows the Arrhenius law. The activation parameters are in accord with expectation, with log A in the 6–8 range and at E_a values of 1–2 kcal/mol.

In striking contrast, cyclobutanediyls that are devoid of stabilizing substituents decay even at 4 K. Reaction rates are remarkably insensitive to temperature, and quantum mechanical tunneling is involved in the ring closure. A model has been developed to rationalize the contrasting behaviors of stabilized vs fully localized cyclobutanediyls. Delocalizing substituents are thought to deepen the potential energy well in which the singlet biradical lies. This widens the barrier to ring closure and thus suppresses tunneling. The model rationalizes the observed trends in activation parameters and appears to be consistent with cyclopropane thermal rearrangement chemistry.

Analysis of the decay kinetics requires an explicit inclusion of matrix-site effects. This system can be quite well modeled with a Gaussian distribution of activation energies. The magnitude of the matrix effect—as estimated by the standard deviation of the Gaussian—is fairly small, on the order of 1 kcal/mol or less. However, at cryogenic temperatures such small perturbations can produce monumental rate effects. The key requirement for successful simulation is an absolute intensity measurement, i.e., a normalization of the decay curve. Given this, the methodology we have developed should be generally applicable to studies of dispersive kinetics.

Experimental Section

The synthesis of diazenes **2** and the EPR spectroscopy of biradicals **1** have been described in detail elsewhere.[2]

Distribution Slicing. The sample preparation and EPR instrumentation used have been described previously.[2] A strong triplet signal was generated by prolonged photolysis (20 s to 12 min) of the sample in the EPR cavity at 3.8 K. The intensity was recorded continuously throughout the experiment with occasional reference to an off-resonance base line. Care was taken to ensure that the signal was not saturated. At 3.8 K this was only possible for the $\Delta m_s = 2$ transition, typically at power settings of 0.02 mW or less. Warming of the matrix was accomplished either by restricting helium flow or by using the heater and automatic temperature control. In either case, equilibration was completed as quickly as possible without overshooting the desired temperature. Calibration of temperature was generally done before and after the experiment, the experimental temperatures being determined by interpolation of the available calibration points. The intensity after each cycle was measured following reequilibration to 3.8 K.

Decay-Trace Fitting. Decay traces were recorded by first equilibrating the sample in the EPR cavity to the desired temperature, which was determined by calibration immediately before and/or after the trace. With the spectrometer set to the field of the strongest transition, a signal was generated by photolysis through a combination of filters chosen to transmit a narrow band of radiation near 340 nm. Photolysis intervals were controlled by using a Vincent Associates Model SD-10 timed shutter and were kept only as long as necessary to generate an adequate signal. Base-line measurements at an off-resonance field were recorded before the generation and after the decay to allow later correction for any observed drift. The traces were digitized and stored on disk as collected with a Compaq Plus computer. Each data file contained 1000 intensity measurements. Decay traces were normally recorded at a nonsaturating microwave power, but higher power was sometimes used to allow shorter photolyses. No difference was distinguishable between saturated and nonsaturated traces, and the two types were fitted equally well in the analysis.

Acknowledgment. We thank the National Science Foundation for generous support of this work. F.D.C. was supported by a Jet Propulsion Laboratory/Center for Space Microelectronics Technology Fellowship sponsored by the Strategic Defense Initiative Organization/Innovative Science and Technology Office.

Registry No. 1-H, 95580-29-3; **1**-Me, 92937-60-5; **1**-Et, 112422-81-8; **1**-Vin, 112422-86-3; **1**-Ph, 112422-85-2; **1**-EV, 112422-84-1.

Reactions of *N*-Halo-*N*-methylbenzylamines with MeONa–MeOH and *t*-BuOK–*t*-BuOH. Effects of β-Carbon Substituent and Base–Solvent System upon the Imine-Forming Transition State

Richard A. Bartsch*,[1a] and Bong Rae Cho*,[1b]

Contribution from the Department of Chemistry and Biochemistry, Texas Tech University, Lubbock, Texas 79409, and the Department of Chemistry, Korea University, Seoul, Korea.
Received August 1, 1988

Abstract: Elimination reactions of $YC_6H_4CH(R)N(X)CH_3$ in which R = Me and Ph and X = Cl and Br promoted by MeONa–MeOH and *t*-BuOK–*t*-BuOH have been studied kinetically. The elimination reactions are regiospecific, producing only the corresponding *N*-benzylidenemethylamines, and are quantitative when X = Cl. Comparison with published data for R = H reveals that with both base–solvent combinations variation of the β-carbon substituent from Me to H to Ph produces an increase in the ρ value, first an increase and then a decrease in k_H/k_D, and a decrease in k_{Br}/k_{Cl}. When the base–solvent system is changed from MeONa–MeOH to *t*-BuOK–*t*-BuOH, the ρ value increases, k_H/k_D remains nearly constant, and k_{Br}/k_{Cl} decreases for all three R groups. From these results, the changes in transition-state structure wrought by variation of the β-carbon substituent and the base–solvent system are assessed.

Extensive studies of olefin-forming, 1,2-elimination reactions have led to a detailed understanding of the relationship between E2 transition-state structure and changes in substrate structure, base–solvent combination, and other reaction variables.[2a,3] In

0002-7863/89/1511-2252$01.50/0

Table I. Rate Coefficients for Eliminations from $YC_6H_4CL(CH_3)N(X)CH_3$ Induced by MeONa–MeOH

entry	compd[a]	temp, °C	[MeONa], M	10^2k_2,[b] M^{-1} s^{-1}
1	**1a**	29.6	0.0995	0.366 ± 0.003
2	**1a**	39.0	0.00398	1.06 ± 0.01
3	**1a**	39.0	0.0995	1.00 ± 0.00
4	**1b**	39.0	0.0995	0.223 ± 0.001
5	**1c**	39.0	0.105	28.8 ± 0.4
6	**1a**	48.5	0.0995	2.43 ± 0.04
7	**1d**	39.0	0.0995	0.679 ± 0.037
8	**1e**	39.0	0.0995	1.13 ± 0.02
9	**1f**	39.0	0.0995	0.684 ± 0.005
10	**1h**	39.0	0.0995	2.67 ± 0.13
11	**1j**	39.0	0.0995	4.21 ± 0.00
12	**1k**	39.0	0.105	5.70 ± 0.05
13	**1l**	39.0	0.105	115 ± 6
14	**1m**	39.0	0.00995	43.4 ± 0.6
15	**1n**	39.0	0.00995	15.3 ± 0.6

[a] [Substrate] = 8–13 × 10^{-5} M. [b] Average rate coefficient and standard deviation from the average for two or more kinetic runs.

Table II. Rate Coefficients for Eliminations from $YC_6H_4CL(CH_3)N(X)CH_3$ Induced by *t*-BuOK–*t*-BuOH

entry	compd[a]	temp, °C	[*t*-BuOK], M	10^2k_2,[b] M^{-1} s^{-1}
1	**1a**	29.6	0.0134	3.09 ± 0.04[b]
2	**1a**	39.0	0.0128	6.45 ± 0.02
3	**1a**	39.0	0.0134	6.74 ± 0.02
4	**1a**	39.0	0.0511	6.95 ± 0.04
5	**1a**	39.0	0.0950	6.66 ± 0.14
6	**1b**	39.0	0.0134	1.49 ± 0.04
7	**1c**	39.0	0.0128	97.6 ± 7.6
8	**1a**	48.5	0.0134	13.2 ± 0.2
9	**1d**	39.0	0.0134	3.47 ± 0.01
10	**1e**	39.0	0.0134	9.53 ± 0.21
11	**1f**	39.0	0.0134	4.80 ± 0.22
12	**1h**	39.0	0.0134	17.2 ± 0.1
13	**1j**	39.0	0.0134	24.6 ± 0.0
14	**1k**	39.0	0.0202	37.8 ± 0.1
15	**1k**	39.0	0.00410	39.2 ± 1.2
16	**1l**	39.0	0.00410	306 ± 8
17	**1m**	39.0	0.0128	505 ± 2
18	**1n**	39.0	0.01218	149 ± 8

[a] [Substrate] = 8–23 × 10^{-5} M. [b] Average rate coefficient and standard deviation from the average for two or more kinetic runs.

contrast, much less is known concerning base-promoted, 1,2-elimination reactions which form carbon–nitrogen double bonds.[2b,4-16]

In earlier work, we have investigated eliminations from *N*-chloro- and *N*-bromo-*N*-alkylbenzylamines induced by MeO-Na–MeOH, *t*-BuOK–*t*-BuOH, and R_2NH–MeCN to determine the effects of leaving group and base–solvent system variation and steric interactions of α-alkyl groups upon the imine-forming transition state.[8-12] Comparison of the results with those for closely related, olefin-forming eliminations reveals both similarities and differences for the two types of elimination reactions.

To further expand our understanding of imine-forming elimination mechanisms, reactions of β-substituted *N*-halo-*N*-methylbenzylamines **1** and **2** with MeONa–MeOH and *t*-BuOK–*t*-BuOH (eq 1) have now been studied. When combined with existing data for the parent *N*-halo-N-methylbenzylamines (**3**),[8] the results establish the effect of introducing an electron-donating (Me) and an electron-withdrawing (Ph) group at the β-carbon in the imine-forming transition state. Also the studies reveal the comparative influence of base–solvent combination variation from MeONa–MeOH to *t*-BuOK–*t*-BuOH as substitutions are made at the β-carbon. The results are interpreted with a More O'Ferrall–Jencks reaction coordinate diagram.[17]

Table III. Rate Coefficients for Eliminations from $YC_6H_4CL(Ph)N(X)CH_3$ Induced by MeONa–MeOH

entry	compd[a]	temp, °C	[MeONa], M	10^2k_2,[b] M^{-1} s^{-1}
1	**2a**	29.6	0.105	2.45 ± 0.06
2	**2a**	39.0	0.0105	5.73 ± 0.17
3	**2a**	39.0	0.105	5.74 ± 0.18
4	**2b**	39.0	0.105	1.12 ± 0.03
5	**2c**	39.0	0.105	63.6 ± 0.6
6	**2a**	48.5	0.105	12.4 ± 0.2
7	**2d**	39.0	0.105	3.70 ± 0.01
8	**2f**	39.0	0.105	4.29 ± 0.04
9	**2g**	39.0	0.105	4.39 ± 0.05
10	**2h**	39.0	0.105	17.9 ± 0.6
11	**2i**	39.0	0.105	18.6 ± 0.3
12	**2j**	39.0	0.0105	25.6 ± 1.0
13	**2k**	39.0	0.0105	36.3 ± 0.7
14	**2m**	39.0	0.0105	259 ± 1
15	**2n**	39.0	0.0105	108 ± 1

[a] [Substrate] = 3–10 × 10^{-5} M. [b] Average rate coefficient and standard deviation from the average for two or more kinetic runs.

Table IV. Rate Coefficients for Eliminations from $YC_6H_4CL(Ph)N(X)CH_3$ Induced by *t*-BuOK–*t*-BuOH

entry	compd[a]	temp, °C	[*t*-BuOK], M	k_2,[b] M^{-1} s^{-1}
1	**2a**	29.6	0.0293	0.257 ± 0.003[b]
2	**2a**	39.0	0.00202	0.414 ± 0.014
3	**2a**	39.0	0.0140	0.469 ± 0.007
4	**2a**	39.0	0.0293	0.441 ± 0.002
5	**2a**	39.0	0.117	0.427 ± 0.001
6	**2b**	39.0	0.140	0.101 ± 0.004
7	**2c**	39.0	0.00202	3.28 ± 0.06
8	**2a**	48.5	0.0293	0.792 ± 0.027
9	**2d**	39.0	0.0293	0.386 ± 0.008
10	**2f**	39.0	0.0293	0.328 ± 0.008
11	**2g**	39.0	0.0293	0.338 ± 0.008
12	**2h**	39.0	0.0293	1.36 ± 0.01
13	**2i**	39.0	0.0293	1.46 ± 0.03
14	**2j**	39.0	0.0293	1.82 ± 0.06
15	**2k**	39.0	0.0140	2.65 ± 0.06
16	**2k**	39.0	0.00101	1.94 ± 0.01
17	**2l**	39.0	0.0101	13.9 ± 0.2
18	**2m**	39.0	0.00202	22.2 ± 0.2
19	**2n**	39.0	0.00202	10.2 ± 0.3

[a] [Substrate] = 3–10 × 10^{-5} M. [b] Average rate coefficient and standard deviation from the average for two or more kinetic runs.

Results

Reactions of *N*-chloroamines **1a,b,d–k,m,n**, **2a,b,d–k,m,n**, and **3k** with MeONa–MeOH and *t*-BuOK–*t*-BuOH produced only the corresponding imines **4a,b,d–k,m,n**, **5a,b,d–k,m,n**,[18] and **6k**,

(1) (a) Department of Chemistry and Biochemistry, Texas Tech University. (b) Department of Chemistry, Korea University.
(2) Saunders, W. H., Jr.; Cockerill, A. F. *Mechanism of Elimination Reactions*; Wiley-Interscience: New York, 1973: (a) pp 1–200 and (b) pp 484–498.
(3) Cockerill, A. F.; Harrison, R. G. *The Chemistry of Double-Bonded Functional Groups*; Patai, S. Ed.; Wiley-Interscience: New York, 1977; Supplement A, Part 1: (a) pp 149–222 and (b) p 725.
(4) Brauman, S. K.; Hill, M. E. *J. Am. Chem. Soc.* **1967**, *89*, 2131–2135.
(5) Brauman, S. K.; Hill, M. E. *J. Org. Chem.* **1969**, *34*, 3381–3384.
(6) Oae, S.; Sakuri, T. *Bull. Chem. Soc. Jpn.* **1976**, *49*, 730–736.
(7) Bartsch, R. A.; Cho, B. R. *J. Org. Chem.* **1979**, *44*, 145–146.
(8) Bartsch, R. A.; Cho, B. R. *J. Am. Chem. Soc.* **1979**, *101*, 3587–3591.
(9) Cho, B. R.; Yoon, J. C.; Bartsch, R. A. *J. Org. Chem.* **1985**, *50*, 4943–4946.
(10) Cho, B. R.; Namgoong, S. K.; Kim, T. R. *J. Org. Chem.* **1986**, *51*, 1320–1324.
(11) Cho, B. R.; Namgoong, S. K.; Kim, T. R. *J. Chem. Soc., Perkin Trans 2* **1987**, 853–856.
(12) Cho, B. R.; Maeng, J. H.; Yoon, J. C.; Kim, T. R. *J. Org. Chem.* **1987**, *52*, 4752–4756.
(13) Cho, B. R.; Pyun, S. Y.; Kim, T. R. *J. Am. Chem. Soc.* **1987**, *109*, 8041–8044.
(14) Hoffman, R. V.; Cadena, R. *J. Am. Chem. Soc.* **1977**, *99*, 8226–8232.
(15) Hoffman, R. V.; Belfore, E. L. *J. Am. Chem. Soc.* **1979**, *101*, 5687–5692.
(16) Hoffman, R. V.; Belfore, E. L. *J. Am. Chem. Soc.* **1982**, *104*, 2183–2190.
(17) Lowry, T. H.; Richardson, K. S. *Mechanism and Theory in Organic Chemistry*; Harper & Row: New York, 1981: (a) pp 199–205, and (b) pp 542–545.

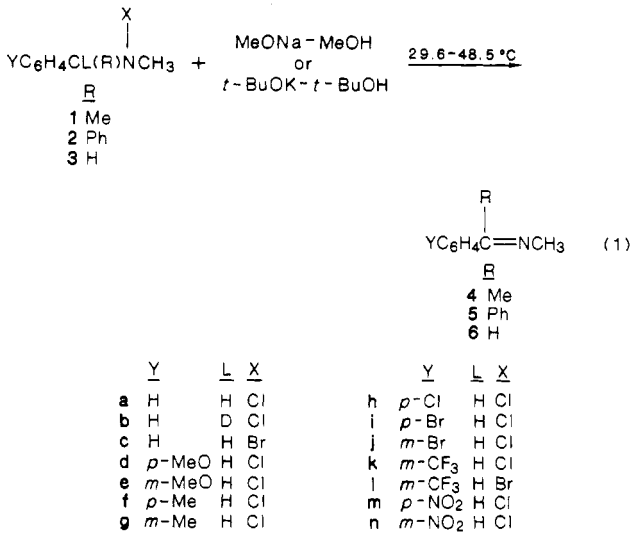

	Y	L	X
a	H	H	Cl
b	H	D	Cl
c	H	H	Br
d	p-MeO	H	Cl
e	m-MeO	H	Cl
f	p-Me	H	Cl
g	m-Me	H	Cl
h	p-Cl	H	Cl
i	p-Br	H	Cl
j	m-Br	H	Cl
k	m-CF_3	H	Cl
l	m-CF_3	H	Br
m	p-NO_2	H	Cl
n	m-NO_2	H	Cl

respectively. Eliminations were followed by monitoring the appearance of absorption at the λ_{max} for the imine products. Excellent pseudo-first-order kinetic plots were obtained which covered at least 3 half-lives. Dividing the pseudo-first-order rate constants by the base concentrations provided the second-order rate coefficients presented in Tables I–V.

The rate coefficients recorded in Table I–IV demonstrate that the reactions are first order in base and first order in substrates. Second-order rate coefficients for reactions of **1a** and **2a** with MeONa–MeOH and *t*-BuOK–*t*-BuOH were constant for 7–50-fold variations in base concentration.

For β-substituent variation, the relative rates of dehydrohalogenation from $C_6H_5CH(R)N(Cl)CH_3$ induced by MeONa–MeOH and *t*-BuOK–*t*-BuOH are Me < H < Ph and Me < Ph ~ H, respectively (Table VI). A statistical correction was applied for the parent compound *N*-chloro-*N*-methylbenzylamine.

Rates of elimination from **1a** and **2a** promoted by MeONa–MeOH and *t*-BuOK–*t*-BuOH were measured at three temperatures spanning 20 °C. Arrhenius plots were linear with excellent correlation coefficients ($r \geq 0.999$). Calculated enthalpies and entropies of activation for eliminations from **1a** and **1b** are compared with those for *N*-chloro-*N*-methylbenzylamine[8] in Table VII.

The influence of aryl group substituents upon rates for reactions of **1** with MeONa–MeOH and *t*-BuOK–*t*-BuOH correlate satisfactorily with the Hammett equation using σ^- values (Figure 1). However, for reactions for **2**, the elimination rates for **2m** (Y = *p*-NO_2) exhibit a large negative deviation from the correlation line for the other substituents (Figure 2). Presumably steric hindrance to coplanarity of the p orbitals of the developing carbanion, the β-phenyl group, and the aromatic ring which contains the *p*-NO_2 group reduce the stabilization of the developing carbanion by resonance interaction with the *p*-NO_2 group. Therefore, the elimination rates for **2m** correlate with neither the σ (triangles) nor σ^- (squares) values in Figure 2 but lies between them. Anomalous behavior has been reported by others for eliminations from a structurally related substrate.[20] For reactions of **2a,d–k,m,n** with MeONa–MeOH and *t*-BuOK–*t*-BuOH, Hammett values were calculated without the data for **2d** and **2m**. Hammett values for reactions of **1a,e–k,n** and **2a,e–k,n** with MeONa–MeOH and *t*-BuOK–*t*-BuOH are compared with those reported for *N*-chloro-*N*-methylbenzylamine[8] in Table VIII.

From the rate data for eliminations from **1a,b** and **2a,b** induced by MeONa–MeOH and *t*-BuOK–*t*-BuOH, values for the primary kinetic deuterium isotope effect were calculated and are compared with values reported for **3a,b** in Table IX.

Reactions of β-substituted *N*-bromo-*N*-methylbenzylamines **1c, 1l, 2c, 2l,** and **3l** with MeONa–MeOH and *t*-BuOK–*t*-BuOH were also examined. The products were mixtures of the corresponding imines and amines. The amine products apparently arose from nucleophilic displacement on the bromine of the substrate by the alkoxide ion.[9] The overall second-order rate constants were multiplied by the imine yields to obtain the rate constants for imine formation. The leaving group effect values, k_{Br}/k_{Cl}, for eliminations from **1–3** are summarized in Table X.

Table V. Rate Coefficients for Eliminations from $YC_6H_4CH_2N(X)CH_3$ Induced by MeONa–MeOH at *t*-BuOK–*t*-BuOH at 39.0 °C

entry	compd[a]	base–solvent	[base], M	10^2k_2,[b] M^{-1} s^{-1}
1	**3k**	MeONa–MeOH	0.105	18.5 ± 0.1
2	**3l**	MeONa–MeOH	0.105	150 ± 1
3	**3k**	*t*-BuOK–*t*-BuOH	0.0140	5.41 ± 0.08
4	**3l**	*t*-BuOK–*t*-BuOH	0.00101	43.4 ± 1.0

[a] [Substrate] = 3–13 × 10^{-5} M. [b] Average rate coefficient and standard deviation from the average for two or more kinetic runs.

Table VI. Relative Rates for Base-Promoted Dehydrochlorination of $C_6H_5CH(R)N(Cl)CH_3$ at 39.0 °C

	relative rate when R is		
base–solvent	Me	H[a]	Ph
MeONa–MeOH	0.5	1.0	3.1
t-BuOK–*t*-BuOH	0.1	1.0	0.9
k(*t*-BuOK)/k(MeONa)	6.7	28[a]	7.7

[a] Data from ref 8.

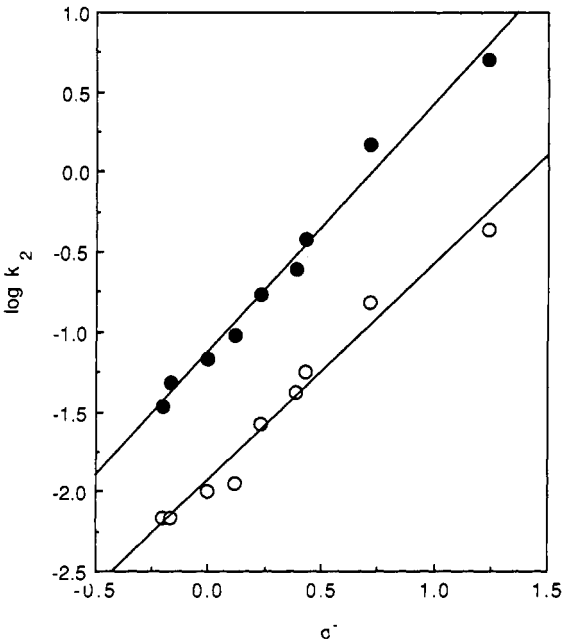

Figure 1. Hammett plots for eliminations from $ArCH(CH_3)N(Cl)CH_3$ promoted by MeONa–MeOH (○) and *t*-BuOK–*t*-BuOH (●).

Discussion

Relative Rates of Elimination for 1–3. The kinetic investigation and control experiment clearly establish that the reactions of **1** and **2** with MeONa–MeOH and *t*-BuOK–*t*-BuOH proceed via an E2 mechanism. Since **1** and **2** were stable in MeOH and *t*-BuOH and the reactions exhibited second-order kinetics, all but

(18) Since the proportion of anti isomers in the equilibrium mixtures of **5h** and **5m** are 58% and 70%,[19] respectively, there is a possibility that a mixture of syn and anti products in varying ratios is produced for reactions of **2c–n** with MeONa–MeOH and *t*-BuOK–*t*-BuOH. However, the excellent linearity of the pseudo-first-order kinetic plots which covered over 3 half-lives indicates that the two competing elimination pathways leading to the isomeric imine products must proceed at the same rate. This is not surprising since the energies of the isomeric reactants and the transition states leading to the two products should be nearly identical because the Ar and Ph groups differ only by a substituent attached to meta or para position in the former. Therefore, conclusions concerning the influence of β-substituent upon the imine-forming elimination would not be affected by the presence of two competing reaction pathways leading to the syn and anti imine products.

(19) Curtin, D. Y.; Hauser, J. W. *J. Am. Chem. Soc.* **1961**, *83*, 3474–3481.

(20) Kice, J. L.; Weclas, L. *J. Org. Chem.* **1985**, *50*, 32–39.

Table VII. Activation Parameters for Base-Promoted Dehydrochlorination of $C_6H_5CH(R)N(Cl)CH_3$

	R = Me		R = H[a]		R = Ph	
base–solvent	$\Delta H^{\ddagger}$	$\Delta S^{\ddagger}$	$\Delta H^{\ddagger}$	$\Delta S^{\ddagger}$	$\Delta H^{\ddagger}$	$\Delta S^{\ddagger}$
MeONa–MeOH	19.2 ± 0.1	−6.4 ± 0.1	16.6	−12.1	16.3 ± 0.1	−11.6 ± 0.1
t-BuOK–*t*-BuOH	14.6 ± 0.2	−17.3 ± 0.6	11.7	−21.1	11.1 ± 0.6	−25.5 ± 2.0

[a] Data from ref 8.

Table VIII. Effect of R Group upon Hammett ρ Values for Base-Promoted Eliminations from $C_6H_5CH(R)N(Cl)CH_3$ at 39.0 °C

	ρ value		
base–solvent	R = Me	R = H[a]	R = Ph
MeONa–MeOH	1.36 ± 0.09	1.52	1.67 ± 0.09
t-BuOK–*t*-BuOH	1.55 ± 0.08	1.68	1.73 ± 0.11

[a] Data from ref 8.

Table IX. Effects of the R Group upon the Deuterium Isotope Effect for Base-Promoted Eliminations from $C_6H_5CH(R)N(Cl)CH_3$ at 39.0 °C

	k_H/k_D		
base–solvent	R = Me	R = H[a]	R = Ph
MeONa–MeOH	4.4 ± 0.1	6.0	5.1 ± 0.3
t-BuOK–*t*-BuOH	4.5 ± 0.1	5.9	4.6 ± 0.2

[a] Data from ref 8.

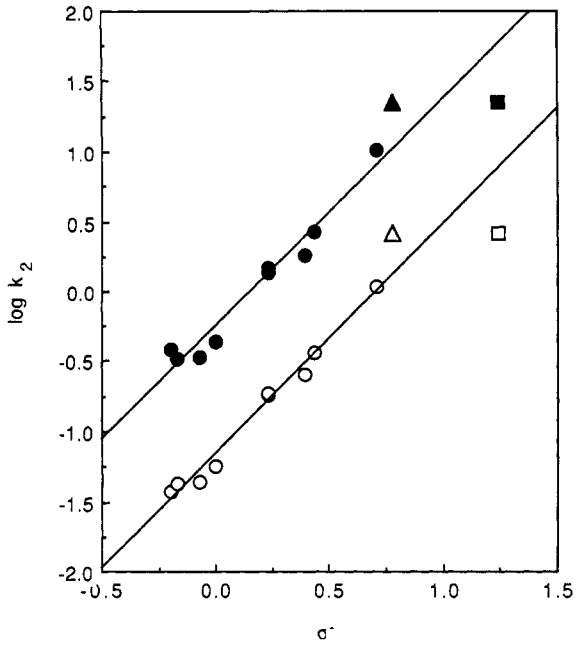

Figure 2. Hammett plots for eliminations from $ArCH(Ph)N(Cl)CH_3$ promoted by MeONa–MeOH (○) and *t*-BuOK–*t*-BuOH (●). (△ and □ are points for log k_2 vs σ and σ^- for *p*-NO_2, respectively.)

bimolecular pathways can be ruled out. In addition, the $(E1cb)_{ip}$ and $(E1cb)_{irr}$ mechanisms are negated by the substantial values for the primary deuterium isotope effect and the element effect of the leaving group (Tables IX and X),[3b] respectively.

The rates of elimination from $YC_6H_4CH(R)N(Cl)CH_3$ promoted by MeONa–MeOH increase with β-substituent variation in the order of Me < H < Ph. A methyl group on the β-carbon atom could stabilize the developing double bond character in the transition state[21] and thereby enhance the rate. On the other hand, it may also retard the rate by decreasing the C_β–H bond acidity[23] and increasing steric hindrance in the substrate.[12,25] Therefore, the observed slower rate of elimination when R = Me compared with R = H may result from decreased C_β–H bond activity and/or increased steric hindrance.

The relative importance of the steric and electronic effects of the β-substituent is demonstrated for R = Ph. A phenyl group would be expected to increase the rate by enhancing the stability of the C=N bond[21] and the acidity of the C_β–H bond.[23] However, its steric effect, which is similar to that of a methyl group,[25] would be anticipated to decrease the rate. Therefore, the observed enhanced rate of elimination when R = Ph compared with R = H suggests that electronic effects of β-carbon substituents are more important than their steric effects in determining the rates of eliminations from **1–3**.

A similar conclusion is reached from consideration of the effect of the base–solvent combination upon the reaction rate. Variation of the base–solvent system from MeONa–MeOH to *t*-BuOK–*t*-BuOH should increase both the base strength and base steric effect, which would have opposing influences upon the rate. With *t*-BuOK–*t*-BuOH, more rapid elimination reactions were observed compared with MeONa–MeOH (Table VI) which clearly demonstrates that the base strength effect is dominant. The diminished $\Delta H^{\ddagger}$ and $\Delta S^{\ddagger}$ values calculated for *t*-BuOK–*t*-BuOH (Table VII) are also consistent with this view. A stronger base would facilitate the base-proton bond formation in the transition state and lower both $\Delta G^{\ddagger}$ and $\Delta S^{\ddagger}$ values, whereas an opposite trend would be anticipated if a base steric affect were important.[12]

It is interesting to note that the $k(t\text{-BuOK})/k(\text{MeONa})$ ratios for **1** and **2** are smaller than that for **3** in which the β-carbon substituent would have the smallest steric effect. Whether the smaller ratios for **1** and **2** result from a change in transition-state character or steric interactions between the larger base and β-carbon substituents cannot be ascertained at present.

Effects of β-Carbon Substituent and Base–Solvent Combination Variation upon the Imine-Forming Transition States. The transition-state parameters for eliminations from **1–3** indicate that there are small but distinct changes in transition-state structure with variation of the β-carbon substituent. For eliminations from **1–3** promoted by MeONa–MeOH and *t*-BuOK–*t*-BuOH, the ρ value increases gradually as the β-substituent is varied in the order Me < H < Ph (Table VIII). Thus, carbanionic character at the β-carbon is found to increase with the carbanion-stabilizing ability of the substituent.

The primary deuterium isotope effect indicates the extent to which the benzylic proton is transferred to the base in the transition state. For eliminations from **1–3**, the k_H/k_D value first increases and then decreases as the β-substituent is changed from Me to H to Ph in both base–solvent systems. Since the deuterium isotope effect has been demonstrated to increase to the maximum and then decrease as the degree of C_β–H bond rupture increases,[10,26] the present result may be interpreted as either a decrease or an increase in the extent of proton transfer in the transition state for a better carbanion-stabilizing β-substituent. However, the latter interpretation is more compatible with the increased ρ values.

The leaving group element effect, k_{Br}/k_{Cl}, indicates the relative extent of N_α–X bond rupture in the transition state. As the degree of N_α–X bond cleavage in the transition state decreases, k_{Br}/k_{Cl}

(21) The K_{eq} values for $Me(Ph)CHN{=}CAr_2 \rightleftharpoons Me(Ph)C{=}NCH(Ar)_2$ and $Me(Ph)CHN{=}CH(t\text{-Bu}) \rightleftharpoons Me(Ph)C{=}NCH_2\text{-}t\text{-Bu}$ are 1.2 and 14.9, respectively.[22] The results indicate that the effect of Ph and alkyl groups upon the C=N bond stability is similar (upper reaction), and the Ph group stabilizes the C=N bond by K_{eq} = 15 (lower reaction).

(22) Cram, D. J.; Guthrie, R. D. *J. Am. Chem. Soc.* **1965**, *87*, 397–398.

(23) Although the p*Ka*'s of benzylic C–H's of **1–3** are not available in the literature, Gau and Marques[24] found that substitution of Ph for a benzylic H of toluene increased the acidity of remaining benzylic C–H bonds by 4.32 pK_a units, whereas a Me group decreased it by 1.66 pK_a units.

(24) Gau, G.; Marques, S. *J. Am. Chem. Soc.* **1976**, *98*, 1538–1541.

(25) Charton, M. *J. Am. Chem. Soc.* **1975**, *97*, 1552–1556.

Table X. Effects of the R Group and Aryl Group Substituent upon the Leaving Group Effect for Base-Promoted Eliminations from *m*-Y-$C_6H_4CH(R)N(X)CH_3$ at 39.0 °C

	k_{Br}/k_{Cl}					
	R = Me		R = H		R = Ph	
base–solvent	Y = H	Y = CF_3	Y = H[a]	Y = CF_3	Y = H	Y = CF_3
MeONa–MeOH	28.8 ± 0.4	20.2 ± 1.2	11.9	8.1 ± 0.1	11.1 ± 0.5	
t-BuOK–*t*-BuOH	15.1 ± 1.1	7.8 ± 0.4	10.8	8.8 ± 0.4	7.9 ± 0.4	7.2 ± 0.3

[a] Data from ref 8.

is expected to diminish because the difference in the leaving group basicity will be reflected to a lesser extent. This prediction is verified by the decrease in k_{Br}/k_{Cl} ratios for **1–3** when Y = H is replaced by Y = *m*-CF_3 (Table X). The electron-withdrawing *m*-CF_3 substituent is expected to acidify the β-hydrogen and shift the transition state toward the E1cb extreme, decreasing the extent of N_α–X bond cleavage in the transition state in agreement with the observed lower k_{Br}/k_{Cl} values. For eliminations from **1–3** promoted by MeONa–MeOH and *t*-BuOK–*t*-BuOH, the k_{Br}/k_{Cl} value decreases gradually as the β-substituent is varied in the order Me > H > Ph. Thus, a decrease in the extent of N_α–X bond cleavage in the transition state is indicated in the same order.

The combined results reveal that the carbanionic character and the extent of C_β–H bond rupture in the transition state increase, but the degree of N_α–Cl bond cleavage decreases, as the β-substituent is changed from Me to H to Ph in both base-solvent systems.

For a given β-carbon substituent, the k_H/k_D value remains nearly constant within experimental error, but ρ increases and k_{Br}/k_{Cl} decreases, for the change from MeONa–MeOH to *t*-BuOK–*t*-BuOH. It appears that in the transition state the extent of C_β–H bond rupture remains nearly the same, but the carbanionic character increases and the degree of N_α–Cl bond cleavage decreases, for this variation of the base–solvent combination.

The changes in transition-state structure with reactant structure variation can readily be rationalized by considering the electronic effects of the β-carbon substituents and the base strength effects of the base–solvent systems[27] in a More O'Ferrall–Jencks reaction coordinate diagram.[17] In previous work, it was established that the transition state for MeONa-promoted elimination from **3** is unsymmetrical with approximately 40% proton transfer, a smaller extent of N_α–Cl bond cleavage, and limited carbanionic character[8-11] which would locate it somewhat toward the upper side from the center in the reaction coordinate diagram (point A in Figure 3). A phenyl group on the β-carbon would lower the energy of the product and the E1cb intermediate.[27] This is expected to shift the transition state toward the product and E1cb intermediate. However, since the effect of β-substituent upon the acidity is greater than that on the double bond stability,[21,23] the perpendicular motion should predominate. Therefore, the effect of a β-Ph group would be to shift the transition state from A to C in Figure 3. This corresponds to more C_β–H bond cleavage, increased carbanionic character, and less N_α–Cl bond rupture, as observed.

Similarly, the presence of a methyl group on the β-carbon would lower the energy of the product but increase the energy of the E1cb intermediate.[27] Since the perpendicular effect is assumed to be predominant (vide supra), the transition state is predicted to move from A to B in Figure 3. Thus, the effect of a β-methyl group would be to decrease the extent of C_β–H bond cleavage and carbanionic character at the β-carbon but to increase N_α–Cl bond scission in the transition state. The prediction is borne out by the decreases in k_H/k_D and ρ values as well as the increase in k_{Br}/k_{Cl} value.

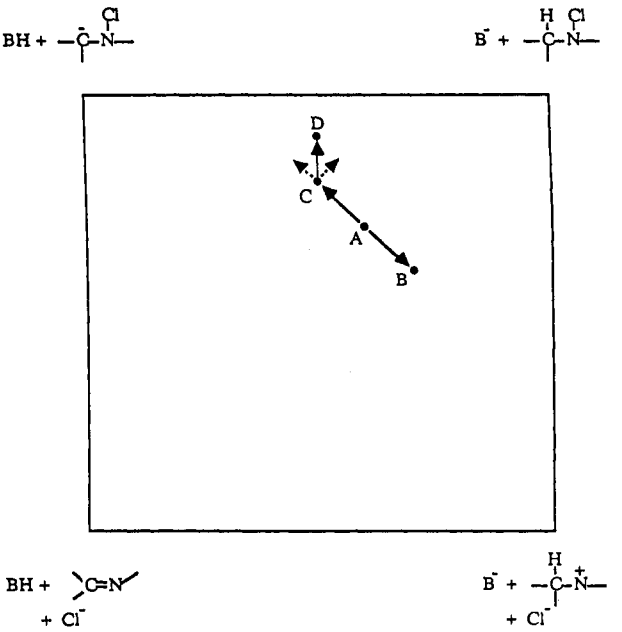

Figure 3. Reaction coordinate energy diagram for base-promoted eliminations from $ArCH(R)N(Cl)CH_3$. Points A, B, C, and D represent the transition states for eliminations from $ArCH_2N(Cl)CH_3$, $ArCH(Me)N(Cl)CH_3$, and $ArCH(Ph)N(Cl)CH_3$ in MeONa–MeOH and $ArCH(Ph)N(Cl)CH_3$ in *t*-BuOK–*t*-BuOH, respectively. Contours and transition states for $ArCH(Me)N(Cl)CH_3$ and $ArCH_2N(Cl)CH_3$ in *t*-BuOK–*t*-BuOH are omitted. Effects of β-carbon substituents and base-solvent upon the transition states position are shown by solid lines.

Variation of the base-solvent combination from MeONa–MeOH to *t*-BuOK–*t*-BuOH increases the base strength,[27] lowering the energy of the right edge of the diagram. This is expected to shift the transition state toward the reactant and the E1cb intermediate. Assuming similar effects for parallel and perpendicular motion, the transition state will shift directly upward as indicated by the shift from C to D in Figure 3. This corresponds to a similar degree of C_β–H bond cleavage, increased carbanionic character, and decreased N_α–Cl bond rupture. This prediction is consistent with the observed results.

The changes in the transition-state structure with β-substituent variation for eliminations induced by *t*-BuOK–*t*-BuOH can also be explained by using a reaction coordinate diagram similar to that just described for MeONa–MeOH.

The present results confirm our previous conclusion that the reaction of **3** with MeONa–MeOH proceeds via an E2-central type of transition state. Addition of a β-phenyl group shifts the transition state toward E1cb-like, whereas a β-methyl group shifts it toward E1-like in the reaction coordinate diagram. When the base–solvent system is changed from MeONa–MeOH to *t*-BuOK–*t*-BuOH, the transition states are shifted directly upward in the reaction coordinate diagram for all substrates.

Experimental Section

The ^1H NMR spectra were recorded with either a Varian A-60 or EM-360 spectrometer with TMS as the internal standard. Mass spectral data were obtained with a Varian MAT 311 spectrometer operating at an ionizing voltage of 16 eV. IR spectra were recorded with a Perkin-Elmer Model 457 spectrophotometer. UV spectra were taken with a Beckman Acta V ultraviolet spectrophotometer with thermostated cuvette

(26) Smith, P. J. *Isotopes of Organic Chemistry*; Buncel, E., Lee, C. C., Ed.; Elsevier: Amsterdam, 1976; Chapter 6.

(27) Although the changes in steric and solvent effects with reactant structure variation may also influence the structure of the transition states, these effects are considered to be of lesser importance since the electronic effects of the β-carbon substituents and the base strength effects of the base–solvent systems are demonstrated to be predominant in these reactions (see text).

holders. Elemental analyses were performed by Triangle Chemical Laboratory, Chapel Hill, NC.

Materials. *m*-Bromobenzophenone,[28] *m*-trifluoromethylbenzophenone,[29] *N*-(α-methylbenzylidene)methylamine,[30,31] *N*,α-dimethylbenzylamines,[32] and *N*-(α-arylbenzylidene)methylamines[31] were prepared in high yields by known methods. *N*-Methyl-α-arylbenzylamines were obtained by reducing **5** with $NaBH_4$ in methanol. $PhCD(CH_3)NHCH_3$ was prepared from acetophenone, CH_3NH_2, and $NaBD_3CN$ in methanol.[32] $Ph_2CDNHCH_3$ was obtained by reduction of $Ph_2C{=}NCH_3$ with $NaBD_4$ in methanol. Most of the reactants and products were known compounds which gave ^1H NMR and IR spectra consistent with the proposed structures. For the following new compounds, bp, IR, ^1H NMR, and mass spectral or elemental analysis data are given as Supplementary Material: *N*,α-dimethyl-3-bromobenzylamine; *N*,α-dimethyl-3-nitrobenzylamine: *N*,α-dimethyl-4-nitrobenzylamine; *N*,α-dimethyl-3-trifluoromethylbenzylamine; *N*-methyl-α-phenylbenzylamine; *N*-methyl-α-deuterio-α-phenylbenzylamine; *N*-methyl-α-phenyl-3-bromobenzylamine; *N*-methyl-α-phenyl-4-bromobenzylamine; *N*-methyl-α-phenyl-4-chlorobenzylamine; *N*-methyl-α-phenyl-3-methylbenzylamine; *N*-methyl-α-phenyl-4-methylbenzylamine; *N*-methyl-α-phenyl-3-nitrobenzylamine; *N*-methyl-α-phenyl-4-nitrobenzylamine; *N*-methyl-α-phenyl-3-trifluoromethylbenzylamine; *N*-(α-phenyl-3-bromobenzylidene)methylamine (**5j**); *N*-(α-phenyl-3-methyl-benzylidene)methylamine (**5g**); *N*-(α-phenyl-3-nitrobenzylidene)methylamine (**5n**); *N*-(α-phenyl-3-trifluoromethylbenzylidene)methylamine (**5k**).

N-Halo-*N*-methylbenzylamines were prepared as before.[8] MeONa–MeOH and *t*-BuOK–*t*-BuOH solutions were prepared as previously described.[8]

Utlraviolet Spectra of 4 and 5. Molar extinction coefficients (λ_{max}) were measured in methanol: **4a**, 11 400 (238 nm); **5a**, 14 200 (244 nm); **5d**, 14 400 (265 nm); **5f**, 15 500 (246 nm); **5g**, 14 000 (245 nm); **5h**, 17 200 (249 nm); **5j**, 13 400 (245 nm); **5m**, 22 000 (234 nm); **5n**, 13 200 (278 nm). The λ_{max} values for **4d–n**, **5i**, and **5k** were obtained from the ultraviolet spectra of the infinity samples from preliminary kinetic runs of the eliminations from **1d–n**, **2i**, and **2k**, respectively, promoted by MeONa–MeOH, assuming that the eliminations were quantitative. The results were **4d** (259 nm); **4e** (241 nm); **4f** (243 nm); **4h** (243 nm); **4j** (235 nm); **45** (240 nm). The molar extinction coefficient and λ_{max} values for **4a** and **5a** were found to be the same in both *t*-BuOH and MeOH. It was therefore assumed that the extinction coefficient and λ_{max} values for **4** and **5** were the same in the two solvents.

Kinetic Studies of Eliminations from 1 and 2. Kinetic studies were carried out as before[8] by measuring the appearance of absorption at the λ_{max} of **4** or **5**. The pseudo-first-order rate constants were divided by the base concentration to afford the second-order rate constants, k_2.

Product of Elimination from 1a. For base-promoted elimination from **1a**, the yields of **4a** calculated from the absorbance of infinity samples in the kinetic reactions were 91.7% with MeONa–MeOH and 90.0% with *t*-BuOK–*t*-BuOH, respectively.

The absence of other products from reactions of **1a** with MeONa–MeOH and *t*-BuOK–*t*-BuOH was established by examining the ^1H NMR spectra of the isolated products by using more concentrated reagents as described earlier.[8] The ^1H NMR spectrum of the products from reaction between **1a** and MeONa–MeOH showed clean singlets corresponding to the $N{-}CH_3$ and $C{-}CH_3$ protons of **4a** at δ 3.3 and δ 2.2, respectively, as well as the methyl peak of acetophenone at δ 2.5. The peak ratio indicated that approximately 30% of acetophenone was present in the product mixture. No absorption due to the starting amine or other products could be detected. To determine whether the acetophenone was produced by the hydrolysis of **4a** during the reaction, **4a** was subjected to the same reaction condition, and the ^1H NMR spectrum was examined. The spectrum was nearly identical with that of the elimination product with the presence of about 30% acetophenone. When a drop of water was added to the reaction mixture, acetophenone was obtained as the only product, demonstrating the facility of the hydrolysis reaction. The ^1H NMR spectrum of the products of reaction between **1a** and *t*-BuOK–*t*-BuOH indicated that the same products were obtained as with MeONa–MeOH, but the proportion of acetophenone was less (16%).

Product of Elimination from 2a. For elimination from **2a**, the yields of **5a** determined by UV spectroscopy were 99.1% with MeONa–MeOH and 94.9% with *t*-BuOK–*t*-BuOH, respectively. The ^1H NMR spectrum of the reaction product was identical with that of authentic **5a**. No absorption due to other products was noted in the ^1H NMR spectrum.

Products of Reaction of 1c with MeONa–MeOH and *t*-BuOK–*t*-BuOH. In infinity samples from kinetic studies of the reactions of **1c** with MeONa–MeOH and *t*-BuOK–*t*-BuOH, the yields of **4a** were 60.4% and 58.0%, respectively. The ^1H NMR spectrum of the products from reaction of **1c** with MeONa–MeOH showed absorption corresponding to $N{-}CH_3$ (s, δ 2.3) and $C{-}CH_3$ (d, δ 1.4) protons of the starting amine and methyl protons (s, δ 2.4) of acetophenone. Considering that **4a** is very vulnerable to hydrolysis (vide supra), the presence of acetophenone in the product mixture strongly indicates that **4a** is formed from the reaction. Similarly, the ^1H NMR spectrum of the products of reaction between **1c** and *t*-BuOK–*t*-BuOH indicated the presence of *N*,α-dimethylbenzylamine (**4a**) and acetophenone. Therefore, it is clear that the reactions of **1c** with MeONa–MeOH and *t*-BuOK–*t*-BuOH produce **4a** and the starting amine.

Products of Reactions of 2c with MeONa–MeOH and *t*-BuOK–*t*-BuOH. For reactions of **2c** with MeONa–MeOH and *t*-BuOK–*t*-BuOH, the yields of **5c** determined by UV spectroscopy were 74.1% and 52.3%, respectively. The ^1H NMR spectra of the products indicated that the products were again the corresponding imine and amine.

Control Experiment. Stability of the *N*-haloamines in MeOH and *t*-BuOH was demonstrated by the previously used method.[8]

Acknowledgment. This investigation was supported by the Robert A. Welch Foundation. B.R.C. thanks the Korea Science and Engineering Foundation for financial support.

Registry No. 1a, 118762-10-0; **1c**, 118761-68-5; **1d**, 118761-69-6; **1e**, 118761-70-9; **1f**, 118761-71-0; **1h**, 118761-72-1; **1j**, 118761-73-2; **1j**, X = H, 118761-98-1; **1k**, 118761-74-3; **1k**, X = H, 118761-99-2; **1l**, 118761-75-4; **1m**, 118761-76-5; **1m**, X = H, 118762-00-8; **1n**, 118761-77-6; **1n**, X = H, 118949-34-1; **2a**, 118761-78-7; **2a**, X = H, 14683-47-7; **2b**, 118761-79-8; **2c**, 118761-80-1; **2d**, 118761-81-2; **2f**, 118761-82-3; **2f**, X = H, 118762-02-0; **2g**, 118761-83-4; **2g**, X = H, 118762-03-1; **2h**, 118761-84-5; **2h**, X = H, 118762-04-2; **2i**, 118761-85-6; **2i**, X = H, 118762-05-3; **2j**, 118761-86-7; **2j**, X = H, 118762-06-4; **2k**, 118761-87-8; **2k**, X = H, 118762-07-5; **2l**, 118761-90-3; **2m**, 118761-88-9; **2m**, X = H, 118762-08-6; **2n**, 118761-89-0; **2n**, X = H, 118762-09-7; **4a**, 6907-71-7; **4d**, 118761-91-4; **4e**, 118761-92-5; **4f**, 53370-98-2; **4h**, 118761-93-6; **4j**, 118761-94-7; **4k**, 118797-81-2; **5a**, 13280-16-5; **5d**, 92850-33-4; **5f**, 92850-05-0; **5g**, 118761-95-8; **5h**, 92290-55-6; **5j**, 118761-96-9; **5k**, 118762-01-9; **5m**, 93533-13-2; **5n**, 118761-97-0; D_2, 7782-39-0; MeONa, 124-41-4; *t*-BuOK, 865-47-4.

Supplementary Material Available: Listing of bp, IR, ^1H NMR, and mass spectral or elemental analysis for all new compounds (3 pages). Ordering information is given on any current masthead page.

(28) Vogel, A. I. *Practical Organic Chemistry*, 3rd ed.; Longman: London, 1973; pp 734, 791.
(29) Van der Stelt, C.; Funcke, A. B.; Nauta, W. *Zh. Arzeim. Forsch.* **1964**, *14*, 964–967.
(30) Kyba, A. I. *Org. Prep. Proc.* **1971**, *2*, 149–156.
(31) Moretti, I.; Torre, G. *Synthesis* **1970**, 141.
(32) Borch, R. F.; Bernstein, M. D.; Durst, H. D. *J. Am. Chem. Soc.* **1971**, *93*, 2897–2904.
(33) Two closely spaced singlets corresponding to syn and anti isomers.